Bull. Chem. Soc. Ethiop. **2022**, 36(2), 353-361.
© 2022 Chemical Society of Ethiopia and The Authors
DOI: https://dx.doi.org/10.4314/bcse.v36i2.9

ISSN 1011-3924
Printed in Ethiopia
Online ISSN 1726-801X

SYNTHESIS, CHARACTERIZATION AND STRUCTURAL STUDY OF Fe(III) COMPLEX DERIVED FROM SODIUM DODECYL BENZENE SULFONATE

Zahira Chaieb[1,2], Zahia Zizi[1*] and Abderrezak Benghalem[2]

[1]Laboratory of Advanced Materials and Physicochemistry for Environment and Health, Faculty of Exact Sciences, Djillali Liabes University, 22000 Sidi Bel Abbes, Algeria
[2]Laboratory of Materials Catalysis, Faculty of Exact Sciences, Djillali Liabes University, 22000 Sidi Bel Abbes, Algeria

(Received November 16, 2021; Revised May 11, 2022; Accepted May 12, 2022)

ABSTRACT. Fe(III) complex derived from sodium dodecyl benzene sulfonate (SDBS) has been synthesized and characterized using FT-IR, TGA, UV-Vis and VSM analysis. The complex structure was determined and illustrated. The study of thermogravimetric, optic and magnetic properties are reported and discussed. The bands in electronic spectrum involved a fully allowed transitions characteristic of Charge Transfer absorption from ligand to metal. The structural study revealed an octahedral geometry around the iron(III) ion. The complex obtained has the following formula $[Fe(SDB)_3]11H_2O$, where Fe(III) is linked to three bidentate ligands. This complexation is confirmed by layering FT-IR Ligand/Complex spectra. Moreover, the VSM analysis collected at room temperature exhibits antiferromagnetic behaviour referred to the anti-alignment of the magnetic moment of Fe^{3+}.

KEY WORDS: Sodium dodecyl benzene sulfonate, Iron(III) complex, Spectral analysis, TGA, Magnetic properties

INTRODUCTION

Water is an essential resource for the sustainability of life on earth. With an increase in the population worldwide, the demand for water has escalated in the urban, industrial and agricultural domains [1]. Domestic and industrial laundry wastewater is relatively 'clean' in comparison to other industrial effluents [2]. For over a century, surfactants have been exploited in industrial processes such as detergency, lubrication, corrosion, colloid stabilization, and drug-delivery. Organic components such as linear alkylbenzene sulfonates (LAS) are the most abundant contributing anionic surfactant constituents found in laundry detergents [3-6]. Due to their excellent performance and relatively low cost, LAS are at the same time indispensable and widely used, but their rate in nature is proportionally too. Even, the ubiquity of surfactants monomers in small amount provides their negative impact and spread water pollution. This fact has caught attention of the academic community and raised their interest to remove them using different methods like: adsorption [7], electrochemical degradation [8], ultrasonic irradiation [9] and decomposition by ozonation [10, 11]. According to their charge, surfactants are classified as non-ionic and ionic (anionic, cationic or zwiterionic). Anionic surfactants constitute about 60% of the total surfactant production [12]. Sodium dodecyl benzene sulfonate (SDBS) was used as a typical example of anionic surfactants. SDBS is a major constituent of some synthetic detergents with billions of kilograms produced and dispersed in the environment annually. It has now reached a prominent role in the emerging field of nanotechnology for possible uses in exfoliating graphitic materials [13]. Pradhan *et al.* [14] have developed a highly efficient protocol for the synthesis of a library of chromeno[4,3-b]chromene derivative by applying a Lewis acid-surfactant-combined catalyst (LASC) $[Fe(DS)_3]$. Moreover, Manabe *et al.* [15] have performed several useful carbon-carbon bond-forming reactions in water, using Lewis acid-surfactant-combined catalyst (LASC). These LASCs are composed of water-stable Lewis acidic cations such as scandium and anionic

---

*Corresponding author. E-mail: zahia.zizi@univ-sba.dz, zahiaz@hotmail.com surfactants such as dodecyl sulfate and dodecanesulfonate. In this article, we tried a new approach to minimize the environmental impact of surfactants, especially in aqueous environments. The aim of this work is to trap an anionic surfactant by ferric ions as a stable coordination complex and to determine the properties of the isolated complex.

EXPERIMENTAL

All chemicals were obtained from Sigma-Aldrich and used as received. The solvent used was distilled water. For solubility test, we used EtOH and toluene with a 99.9% purity. The UV-Vis spectra of complex was done using UV-Vis spectrophotometer Specord 210 Plus. A quartz cuvette with a 1 cm path length is used. 8 mg/L of the complex was dissolved in EtOH at room temperature. The spectral scan covered wavelengths from 190 to 1,100 nm. Infrared spectra of ligand and synthesized complex were collected on a FT-IR spectrophotometer Perkin-Elmer Frontier, over 500 to 4000 cm^{-1} range with a resolution of 2 cm^{-1}. Thermogravimetric analysis (TGA) was performed with the thermos-analyser Setaram-Labsys under oxygen atmosphere (0-1,000 °C) for a sample mass of 20.2×10^{-3} g.

Synthesis of complex [Fe(SDB)$_3$]12H$_2$O

The surfactant was dissolved in a minimum volume of solvent at room temperature. The solution should stay overnight to evacuate air bubbles. Metal Chloride was dispersed in a minimum of distilled water and filtered before use. Metal solution was added slowly to the ligand one, maintaining stirring until a precipitate forms according to the method cited in literature [16]. The compound was prepared using 5:1 (M = Fe:L = SDBS) molar ratio. After 72 h of stirring, yellow precipitate was filtered out and thoroughly washed with distilled water. The isolated complex was stored at room temperature in a watch glass under vacuum.

Synthesis conditions and Environment compatibility

The shape of surfactants depends on their concentration and chemical's structure as well as on their environment (temperature, presence of salt, type of solvent and pH variation). To fulfil all surfactants sensitivities, we tried to find the optimum environment. We conducted experiments on specifics conditions. The following parameters deserve mention.

Effect of solvent

Synthesis was performed in distilled water considering the SDBS's hydrophilic affinity as well as the hygroscopic character of metallic ion Fe^{3+}. We expect the presence of finite amount of water explaining the waxy solid obtained.

Effect of temperature (Krafft point)

As indicated earlier, we are interested by surfactants in their hydrated solids state. Knowing that T_{Krafft} of SDBS = 27.6 °C [17], we prepared a surfactant solution at a concentration above CMC (critical micelle concentration) value and at room temperature (20 °C).

Effect of salt

The reaction between SDBS and $FeCl_3$ forms NaCl salt as a by-product. As reported in the literature, the Krafft temperature increased when salt was present in solution [18]. This leads to avoid any formation of micelles.

Effect of pH

The pH of distilled water was 8, that of SDBS was 10 [19] and the initial pH of $FeCl_3$ was 2. The molar ratio was 5:1 (M:L). The complex formation was instantaneous without having to control the pH.

RESULTS AND DISCUSSION

The hydrophobic character of complex may be explained by the formation of a new bond between iron and hydrophilic head of ligand. Solubility of iron complex in toluene (lipophilic solvent), confirmed this new characteristic. It can be explained by the involved of the charged polar head group of SO_3^- with other atoms. The obtained complex dissolved in toluene, has a very low conductivity. The low molar conductance value of the studied complex indicates a non-electrolytic nature [20]. To confirm this neutral charge, we elaborate an electrical circuit with a current of 25.8 mA that turned to zero mA when the complex is connected. This indicates very interesting potential insulation properties.

FT-IR spectrums analysis

FT-IR spectrum of free ligand (Figure 1), shows that the vibration bands of the surfactant can be grouped into two categories: those associated with tail's (dodecyl benzene $C_{12}H_{25}C_6H_4$) and those with sulfonate groups (SO_3^-).

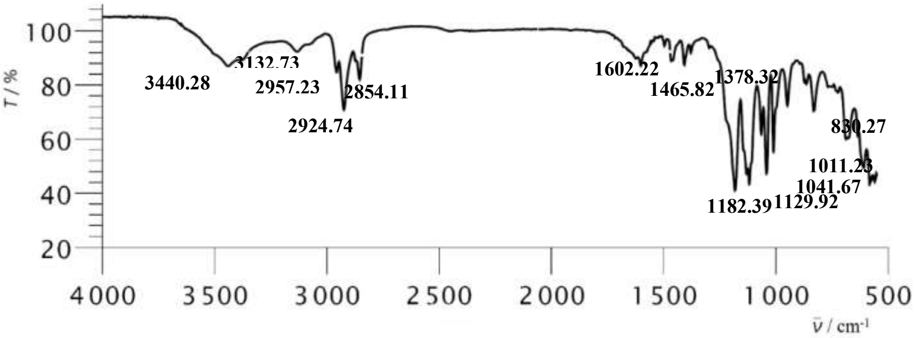

Figure 1. FT-IR spectrum of the SDBS ligand.

The broad band at 3440 $cm^{-1}$is attributed to the O-H bond stretching, indicating the presence of humidity in the ligand. The band at 3132 cm^{-1} is related to C-H stretching for aromatic. The bands at 2924 cm^{-1} and 2854 $cm^{-1}$are attributed to vibration of axial deformation of C-H of the CH_2 group of the surfactant tail.

The band obtained at 2957 cm^{-1} is due to the stretching vibration of the C-H of aromatic. FT-IR wavenumber regions of SDBS and its complex, correlated with the mode of vibration for specific functional groups of ASTM (American Standard of Testing Materials) [21]. This was considered as guideline to characteristic FT-IR absorption bands of LAS. This comparison allowed identifying ligand's significant groups involved in the complex formation.

The ligand functions that do not participate to the complexation phenomenon conserved their frequencies. On comparing, the infrared spectra of the free ligand and the complex, we observed the increase of the band intensity as well as the shift of the S-O band in complex spectrum (Figure 2). The "overlap" noted on sulfonate group in iron complex spectrum (Figure 3), suggests that the ligand is linked to Fe(III) through the oxygen of sulfonate group.

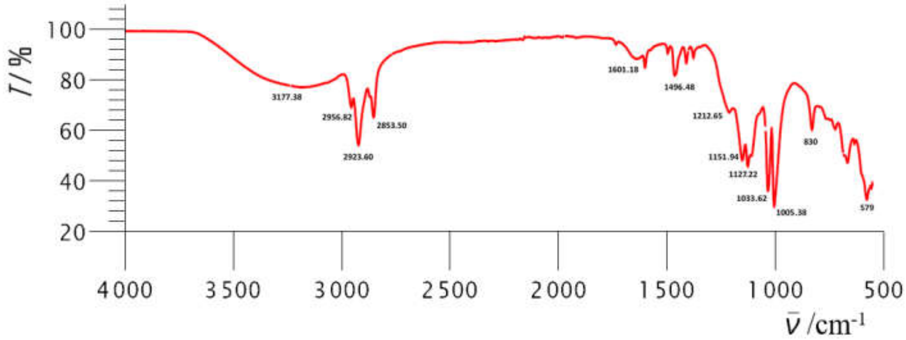

Figure 2. FT-IR spectra of Fe(III) SDBS complex.

Table 1. Principals FT-IR bands of SDBS and its complex.

Functional groups	ν/cm^{-1}		Literature	
	SDBS	[Fe(SDB)$_3$]	SDBS	[Fe(SDB)$_3$]
O-H stretching	3440 (Free-OH)	3177 (Intermolecular bonded)	3280 [22]	-
Alkyl C-H stretching aromatic Stretching C-H of aromatic	3132 2957	- 2956	2960	-
Asymmetric stretching of–CH(CH$_2$) vibration	2924	2923	2917 [23]	-
Symmetric stretching of–CH$_2$(CH$_2$) vibration	2854	2853	2849 [23]	-
Aromatic bands	1465	1496	1494 [24]	-
Aromatic overtones	1600-2000	1600-2000	1667-2000 [24]	-
C=C stretch aromatic	1400-1600	1400-1600	1475-1600 [24]	-
Asymmetric sulfonate group	1420-1330	1420-1330	1235-1176 [21]	-
Symetric sulfonate group	1200-1145	1200-1145	1136 [21]	-
Alkyl benzene sulfonate	1041	1005	1042 [21]	-
Alkyl benzene sulfonate	1011	1033	1010 [21]	-
Para substitution	830	830	833 [21]	-

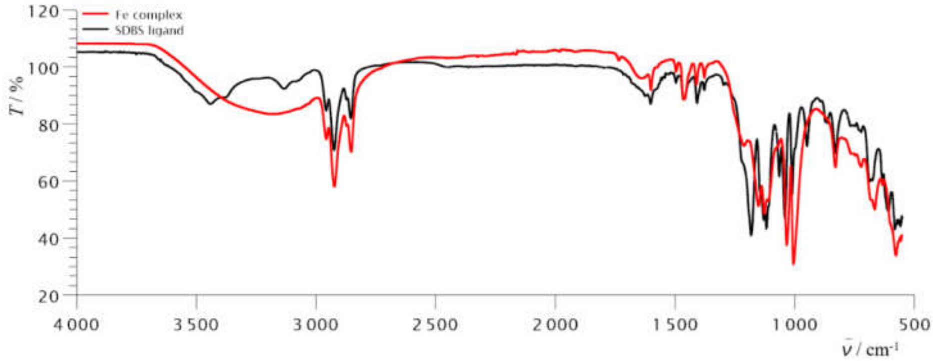

Figure 3. Layering FT-IR ligand/complex spectra.

The absorption bands in the range of 500 to 600 cm^{-1} reveal the presence of metal-oxygen bonds, which can be assigned to the vibrations of Fe-O and O-Fe-O bonding in the octahedral structure as found by Janbutrach *et al.* [25]. According to Bohara *et al.* studies [26], the appearance of a new band at 579 cm^{-1} attributed to the vibration of Fe-O bond confirms the complex formation. The iron metal Fe^{3+} is bonded to SDBS by two oxygen atoms. The ligand acts in its bidentate form. Principals FT-IR bands of SDBS and its complex are listed in Table 1.

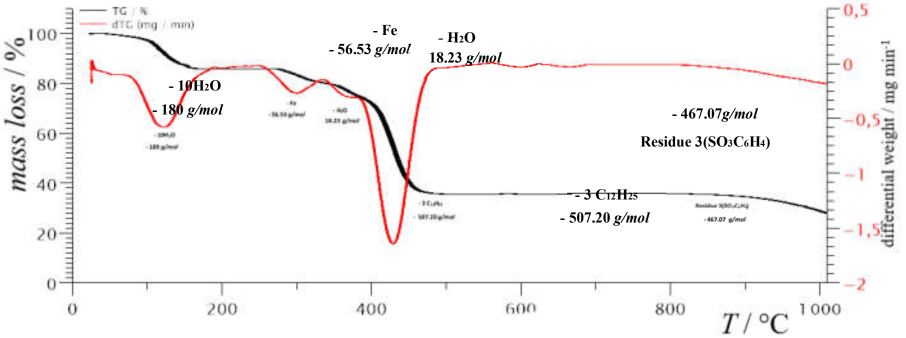

Figure 4. TGA analysis of Fe(III) SDB complex.

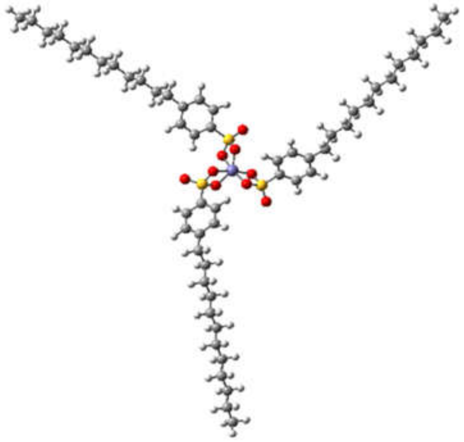

Figure 5. Structure of Fe(III) SDB complex.

TGA analysis

This analysis consolidated the coordination of Fe(III) with 3 ligands (SDB). The presence of an important amount of H_2O (Figure 4), confirms the hygroscopic character of the complex and suggests the presence of 10 molecules of H_2O. During complexation process, the surfactant hydrophilic head was coordinated to the metal. That is why the synthesized complex was agglomerated in aqueous phase and turned out to hydrophobic waxy solid. We also detected one molecule of H_2O liberated around 360 °C probably trapped by the lattice of hydrophobic chains during complexation phenomenon. The iron complex was stable until the temperature of 285 °C. The waste masses provided by TGA analysis (Figure 4), allow calculating molecular weight (180 + 56.53 + 18.23 + 507.20 + 467.07 = 1229.03 g.mol^{-1}). Finally, we suggest the structure $[Fe(DBS)_3]11H_2O$ (Figure 5) for the isolated complex, with a molecular weight of 1229.03 g.mol^{-1}.

Electronic spectroscopy

The electronic spectroscopy is an excellent tool to define the charge nature of $[Fe(SDB)_3]$ complex.

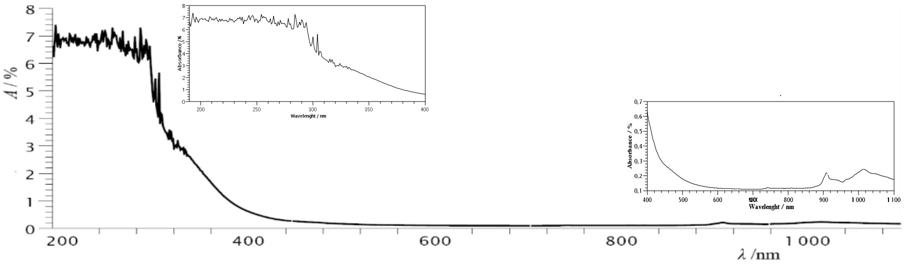

Figure 6. UV-Vis-NIR spectrum of Fe (III) SDBS complex.

The bands between 200–300 nm (Figure 6) are assigned to the allowed transitions of charge transfer ligand metal (CTLM). This large band centred at 300 nm confirms the presence of an octahedral environment around Fe(III). SDBS is a weak ligand, suggesting the following electronic structure $t_2g^3eg^2$. That means that there are many d to d weak transitions in the region (400-800 nm). These transitions are not visible in the UV vis spectrum because of the strong absorption of allowed charge transfer transitions.

According to the works of Schneider *et al.* [27] , Stephens *et al.* [28] and Rada *et al.* [29], the appearance of bands in the region 800–1500 nm is characteristic of a distorted-octahedral high spin Fe(II) complexes. Indeed, Miessler *et al.* [30] have confirmed that for M^{2+} complexes, we must have $\Delta oct = 7,500 - 12,500$ cm^{-1} or $\nu = 800–1,350$ nm. These observations suggest that under irradiations, the ferric ions (Fe^{3+}) were reduced to ferrous (Fe^{2+}).

Vibration sample microscope analysis

The vibrating sample microscope is collected at room temperature for a sample mass of 38.200 10^{-3} g. Figure 7 describes the magnetic behavior of the complex measured by VSM at room temperature. Referred to the magnetic hysteresis (Figure 7), $[Fe(SDB)_3]$ complex exhibits antiferromagnetic behaviour due to the anti-alignment of the magnetic moments of the Fe^{3+} ions. This is in good agreement with the results found in literature [30-32]. Hence, iron complexes follow magnetic phase transition from paramagnetic to anti-ferromagnetic nature at low temperature. The hysteresis loops indicate the dependence of magnetization M on the applied magnetic field H. Magnetic properties of the Fe(III) complex are shown in Table 2.

The coercivity value (Hc = 85.754 G (6.8243 kA/m)); shown in Table 2; suggests that the iron(III) complex has a medium magnetic character. According to Rawlings *et al.* [33], the coercivity value indicates a magnetic character between hard (greater than 10 kA/m) and soft (less than 1 kA/m) materials. The saturation magnetization and retentivity are respectively 0.29908 emu/g and 3.2199 x 10^{-3} emu/g which are considered as small values.

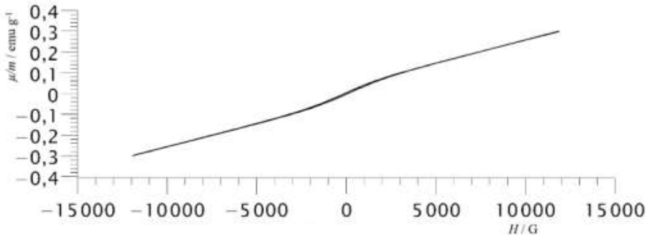

Figure 7. VSM hysteresis loop of $[Fe(SDB)_3]$ complex measured at room temperature.

Table 2. Magnetic properties for iron complex.

Properties	$Fe(SDB)_3$
Coercivity	85.754 *G*
Magnetization	0.29908 emu/g
Retentivity	$3.2199\ 10^{-3}$ emu/g

CONCLUSION

We have successfully trapped the anionic surfactant SDBS, by complexation with iron(III). The synthesized complex was characterized and identified. FT-IR, TGA, UV-Vis and VSM analysis are in good agreement. The spectral study shows that 3 SDB ligands were around Fe(III). The Fe(III) is coordinated to 6 oxygen atoms, suggesting that SDB acts as a bidentate ligand. While UV-Vis spectrum confirms the octahedral coordination and reveals weak d-d transitions. The magnetic hysteresis of VSM analysis exhibits an antiferromagnetic behaviour for the iron(III) complex. The formula of the synthesized hygroscopic complex is $[Fe(SDB)_3]11H_2O$ with a molecular weight of 1229.03 g.mol^{-1}. According to TGA, the iron complex was stable until 285 °C. These thermal, optical and magnetic properties offer a large opportunity for a new SDBS surfactant uses.

REFERENCES

1. Marcucci, M.; Ciardelli, G.; Matteucci, A.; Ranieri, L.; Russo, M.J.D. Experimental campaigns on textile wastewater for reuse by means of different membrane processes. *Desalination* **2002**, 149, 137-143.
2. Schouten, N.; van der Ham, L.G.; Euverink, G.J.W.; de Haan, A.B. Selection and evaluation of adsorbents for the removal of anionic surfactants from laundry rinsing water. *Water Res.* **2007**, 41, 4233-4241.
3. Ramcharan, T.; Bissessur, A. Analysis of linear alkylbenzene sulfonate in laundry wastewater by HPLC–UV and UV–vis spectrophotometry. *J. Surfactants Deterg.* **2016**, 19, 209-218.
4. Duarte, I.; Oliveira, L.L.; Buzzini, A.P.; Adorno, M.A.T.; Varesche, M. Development of a method by HPLC to determine LAS and its application in anaerobic reactors. *J. Braz. Chem. Soc.* **2006**, 17, 1360-1367.
5. Marcomini, A.; Giger, W. Simultaneous determination of linear alkylbenzene sulfonates, alkylphenol polyethoxylates, and nonylphenol by high-performance liquid chromatography. *Anal. Chem.* **1987**, 59, 1709-1715.
6. Villar, M.; Callejón, M.; Jiménez, J.; Alonso, E.; Guiraúm, A. New rapid methods for determination of total LAS in sewage sludge by high performance liquid chromatography (HPLC) and capillary electrophoresis (CE). *Anal. Chim. Acta* **2009**, 634, 267-271.

7. Ni, X.; Li, Z.; Wang, Y. Adsorption characteristics of anionic surfactant sodium dodecylbenzene sulfonate on the surface of montmorillonite minerals. *Front. Chem.* **2018**, 6, 390.
8. Zor, S.; YazicI, B.; Erbi̇l, M.; Galıp, H. The electrochemical degradation of linear alkylbenzene sulfonate (LAS) on platinum electrode. *Water Res.* **1998**, 32, 579-586.
9. Crimi, M.L.; Taylor, J. Experimental evaluation of catalyzed hydrogen peroxide and sodium persulfate for destruction of BTEX contaminants. *Soil Sediment Contam.* **2007**, 16, 29-45.
10. Delanghe, B.; Mekras, C.; Graham, N. Aqueous ozonation of surfactants: A review. *Ozone: Sci. Eng.* **1991**, 13, 639-673.
11. Beltrán, F.; Garcıa, J.; Álvarez, P. Sodium dodecyl benzene sulfonate removal from water ans wastewater. 1. Kinetics of decomposition by ozonation. *Ind. Eng. Chem. Res.* **2000**, 39, 2214-2220.
12. Takayanagi, A.; Kobayashi, M.; Kawase, Y. Removal of anionic surfactant sodium dodecyl benzene sulfonate (SDBS) from wastewaters by zero-valent iron (ZVI): Predominant removal mechanism for effective SDBS removal. *Environ. Sci. Pollut. Res.* **2017**, 24, 8087-8097.
13. Palazzesi, F.; Calvaresi, M.; Zerbetto, F. A molecular dynamics investigation of structure and dynamics of SDS and SDBS micelles. *Soft Matter.* **2011**, 7, 9148-9156.
14. Pradhan, K.; Paul, S.; Das, A.R. Fe (DS) 3, an efficient Lewis acid-surfactant-combined catalyst (LASC) for the one pot synthesis of chromeno [4,3-b] chromene derivatives by assembling the basic building blocks. *Tetrahedron Lett.* **2013**, 54, 3105-3110.
15. Manabe, K.; Mori, Y.; Wakabayashi, T.; Nagayama, S.; Kobayashi, S. Organic synthesis inside particles in water: Lewis acid−surfactant-combined catalysts for organic reactions in water using colloidal dispersions as reaction media. *J. Am. Chem. Soc.* **2000**, 122, 7202-7207.
16. De la Iglesia, P.; Jaeger, V.W.; Xi, Y.; Pfaendtner, J.; Pozzo, L.D. Structure characterization and properties of metal–surfactant complexes dispersed in organic solvents. *Langmuir* **2015**, 31, 9006-9016.
17. Šegota, S.; Heimer, S.; Težak, Đ. New catanionic mixtures of dodecyldimethylammonium bromide/sodium dodecylbenzenesulphonate/water: I. Surface properties of dispersed particles. *Colloids Surf. A Physicochem. Eng. Asp.* **2006**, 274, 91-99.
18. Kolmberg, K.; Jonsson, B.; Kronberg, B.; Lindman, B. *Surfactants and Polymers in Aqueous Solution*, 2nd ed., John Wiley and Sons: New York; **2003**; p 30.
19. Hernandez, O. SIDS Initial Assessment Report For SIAM 20; **2005**.
20. Basu, P.; Nigam, A.; Mogesa, B.; Denti, S.; Nemykin, V.N. Synthesis, characterization, spectroscopy, electronic and redox properties of a new nickel dithiolene system. *Inorg. Chim. Acta* **2010**, 363, 2857-2864.
21. Testing, A.S.F. *Materials, 1983 Annual Book of ASTM Standards: General Products, Chemical Specialties, and End Use Products*. ASTM: USA; **1983**.
22. Sheng, P.X.; Ting, Y.-P.; Chen, J.P.; Hong, L. Sorption of lead, copper, cadmium, zinc, and nickel by marine algal biomass: characterization of biosorptive capacity and investigation of mechanisms. *J. Colloid Interface Sci.* **2004**, 275, 131-141.
23. Viana, R.B.; da Silva, A.B.; Pimentel, A.S. Infrared spectroscopy of anionic, cationic, and zwitterionic surfactants. *Adv. Phys. Chem.* **2012**, 13, 7980-7993.
24. Silverstein, R.M.; Bassler, G.C. Spectrometric identification of organic compounds. *J. Chem. Educ.* **1962**, 39, 546.
25. Janbutrach, Y.; Hunpratub, S.; Swatsitang, E. Ferromagnetism and optical properties of La 1− x Al x FeO 3 nanopowders. *Nanoscale Res. Lett.* **2014**, 9, 1-7.
26. Bohara, R.A.; Thorat, N.D.; Yadav, H.M.; Pawar, S.H. One-step synthesis of uniform and biocompatible amine functionalized cobalt ferrite nanoparticles: a potential carrier for biomedical applications. *New J. Chem.* **2014**, 38, 2979-2986.
27. Schneider, C.; Goktepe, J. *Issues in Emergent Leadership*, John Wiley and Sons: Chicester; **1983**.

28. Stephens, P. *Magnetic Circular Dichroism*, Vol. 35, AIP Publishing: United States of America, **1976**; pp 197-264.
29. Rada, S.; Dehelean, A.; Culea, E. FTIR, Raman, and UV-Vis spectroscopic and DFT investigations of the structure of iron–lead–tellurate glasses. *J. Mol. Model.* **2011**, 17, 2103-2111.
30. Miessler, G.L.; Fischer, P.J.; Tarr, D.A. *Inorganic Chemistry*, 5th ed.; Pearson Education: India; **2008**.
31. Yang, J.; Zhao, L.; Zhang, Y.; Wang, Y.; Liu, H.; Wei, M. Structure and magnetic properties of Mn-doped ZnO semiconductors. *Solid State Commun.* **2007**, 143, 566-569.
32. Mishra, A.; Sharma, R.; Shrivastava, B. Spectroscopic studies on transition metal iron complexes of 2-(N-aryl ethanimidoyl) phenol as ligands. *Indian J. Pure Appl. Phys.* **2011**, 49, 740-747.
33. Rawlings, R.D. *Materials Science And Engineering*, Volume II, EOLSS Publications: Oxford, United Kingdom; **2009**; p 65.